BL39XU
(Magnetic Materials)

1. Introduction

BL39XU is a hard X-ray beamline dedicated to the study of magnetic materials and strongly correlated systems. Techniques include X-ray absorption spectroscopy (XAS), X-ray magnetic circular dichroism (XMCD), X-ray emission spectroscopy (XES), and resonant X-ray magnetic scattering. Our recent developments have supported X-ray spectroscopy measurements under multiple extreme conditions and scanning XAS/XMCD imaging using a nano-focused X-ray beam. These techniques are available for user experiments, and further developments are ongoing. In FY2018, (1) additional analyzer goniometers of the XES spectrometer were installed to complete the mechanical system for 15 crystals and an auto-tuning program of analyzer crystals was developed, (2) the electromagnet for XMCD measurements under multiple extreme conditions was upgraded.

2. Experimental station for X-ray spectroscopy under multiple extreme conditions

2-1. X-ray emission spectrometer with multiple analyzer crystals

To study the electronic and magnetic states of strongly correlated electron systems, instrumentations for X-ray spectroscopy under multiple extreme conditions such as high/low temperature, high magnetic field, and high pressure are progressing at BL39XU [1]. Particularly, XES is a powerful tool to obtain detailed information about electronic states such as valence, spin, and coordination states. However, an accurate XES spectrum of trace elements may take a long time to acquire because the emission signals are generally weak. To overcome this problem, we have been developing a high-efficiency XES spectrometer equipped with multiple analyzer crystals since FY2016.

Figure 1 shows a schematic of the XES spectrometer equipped with 15 analyzer crystals to detect X-ray emission signals in a solid angle as large as 100 mSr. The spectrometer has three towers, each of which can mount a set of five analyzer crystals. A dedicated vacuum chamber (not shown) will be installed to provide a vacuum environment for the towers and the analyzer goniometers. The spectrometer was installed in the downstream space of the experimental hutch 1 in December 2017 and opened to users in 2017B. The initial operation began with five analyzer crystals mounted on the central tower. Instead of a vacuum chamber, an acrylic chamber filled with helium gas is placed on

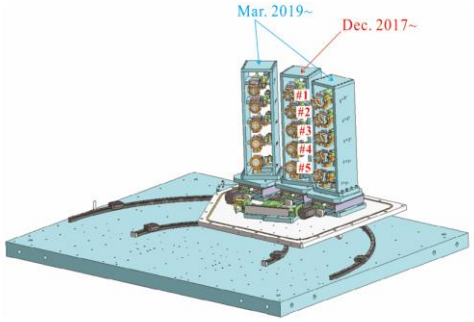

Fig. 1. Schematic of the X-ray emission spectrometer with 15 analyzer crystals. It has three sets of towers, each of which mounts five crystals. All the towers and goniometers can be put into a vacuum chamber. Scattering angles can be changed between 90±60°.

the X-ray paths of sample-to-analyzer and analyzer-to-detector to avoid degradation of X-ray emission intensity. Crystals of Si *nnn*, Si *nn*0, Ge *nnn*, Ge *nn*0, and Ge 331 are available to select the X-ray emission energy.

To further improve the sensitivity and detection efficiency of the XES spectrometer, two goniometer towers each with five analyzer crystals were added on both sides of the existing central tower in March 2019. Thus, the mechanical system of the spectrometer designed for 15 analyzer crystals is now complete. In FY2019, the vacuum chamber will be constructed for the goniometer towers and the 15 crystals will be available with Ge *nnn* crystals. Increasing the number of analyzer crystals may increase the time and complexity of adjusting the spectrometer system. To reduce the adjustment time, software for auto-tuning of the analyzer crystals was developed. Figure 2 shows the spectral profiles of the Eu $L\alpha_1$ emission line in a $Eu_3Fe_5O_{12}$ sample, which was measured with five Ge 333 analyzer crystals automatically tuned with the software.

X-ray beams reflected from the five analyzer crystals are collected by a PILATUS 100K image detector. The angles of the crystals are tuned so that the reflected X-ray beams are placed at nearly the same position on the image detector. Figure 2 shows the profiles of the image intensities integrated over a fixed region [33 pixels (~5.7 mm) in the vertical and 195 pixels (~33.5 mm) in the horizontal directions] as a function of the crystal angle. The result demonstrates that all the profiles exactly overlap. Thus, the software can adjust the angle of analyzer crystals with errors of $< 0.004°$, corresponding to the error in the X-ray emission energy of < 0.1 eV. The current version of the software does not offer an automatic adjustment feature of the focal points of the crystals. We plan to improve the software to extend the auto-tuning function to all 15 analyzer crystals along with a function for a focal point adjustment.

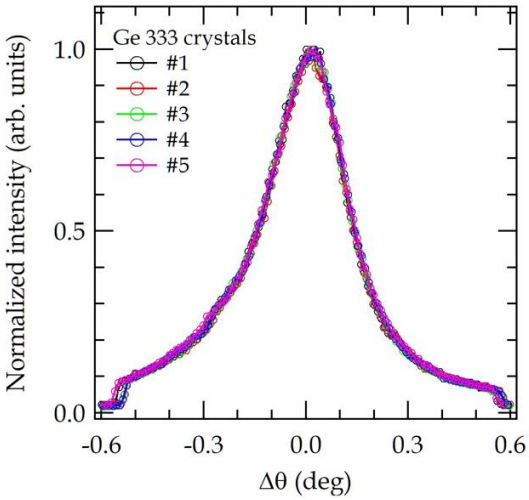

Fig. 2. Scanning result of Ge 333 analyzer crystals after automatic tuning. X-rays at an incident photon energy of 10 keV are irradiated to a $Eu_3Fe_5O_{12}$ sample, and the Eu $L\alpha_1$ ($3d_{5/2}$–$2p_{3/2}$) emission is detected. Origin of the horizontal axis Δθ is a center of emission energy decided by the auto-tuning program.

2-2. High-field electromagnet with a large sample space

X-ray absorption spectroscopy in the hard X-ray region offers a unique opportunity to investigate the electronic and magnetic states of matter under various environments. (strong magnetic field, high/low temperature, and high pressure, etc.) Table 1 shows the sample environments available for X-ray spectroscopy measurement at BL39XU. A dedicated electromagnet is used with cryostat and/or diamond anvil cells (DACs) to generate an environment with a magnetic field of 0.6 T at a temperature of 20 K and pressure up to 200 GPa.

For experiments requiring a higher magnetic field and lower temperature, a superconducting magnet with a miniature DAC (Mini-DAC) is available, and multiple extreme conditions of 7 T, 2 K, and 20 GPa can be produced simultaneously.

The merit of the electromagnet is that it has a sample space (~45 mm) larger than that of the superconducting magnet. This allows the use of a large-size DAC with the electromagnet and provides a much higher pressure. The large sample space makes it easier to build an experimental setup that can combine various kinds of external fields such as an electric field, electric current, and optical lasers. The fast sweeping of the magnetic field is another useful feature of the electromagnet. However, the maximum magnetic field is limited to 0.6 T when used with large DACs.

To enhance the advantage of the experimental setup with the existing electromagnet, a new electromagnet, which can combine an additional large sample space and a magnetic field much higher than that currently available, was installed. Figure 3 shows the new electromagnet. Table 1 compares the features of the existing and new electromagnets and superconducting magnet. The new electromagnet has a high compatibility with existing apparatuses, including the large DAC with nano-polycrystalline diamond anvil cells, high-power 3-K cryostat, high-temperature cryostat (~500 K), and four-element silicon drift detector with high detection efficiency. The use of the new electromagnet allows an expanded sample environment for X-ray spectroscopy under multiple extreme conditions, extending the advantages to high-sensitivity XMCD measurements at BL39XU. This upgrade should inspire research in materials science, magnetism, and spintronics. Potential applications include the development of high-performance permanent magnets with little use of rare earth elements such as Dy, elucidation of the functions of strongly correlated materials, development of spintronics and magnetic storage devices operated under external electric and magnetic fields, and studies on peculiar magnetism

Table 1. Sample environments available for X-ray spectroscopy measurement at BL39XU.

	Existing electromagnet		New electromagnet			Superconducting magnet
Poles gap (mm)	45	10	45	10	5	30 mm (Sample room dia.)
Magnetic field (T)	0.6	2.0	1.5	3.1	3.4	7
Lowest temperature (K)	11 (He-flowing) 3 (Pulse-tube)	20	11 (He-flowing) 3 (Pulse-tube)	20	300	2
Maximum pressure (GPa)	> 170 (300 K) (Large DAC) ~ 40 (11 K) (Mini-DAC)	A.P.	> 170 (300 K) (Large DAC) ~ 40 (11 K) (Mini-DAC)	A.P.	A.P.	~ 40 (Mini-DAC)

Fig. 3. New electromagnet for X-ray spectroscopy experiments under extreme conditions.

emerging under high pressure. The electromagnet was installed in FY2018, and will be available for user experiments in 2019B after commissioning at the Station for X-ray Spectroscopy under multiple extreme conditions.

3. Experimental station for X-ray nanospectroscopy

At the X-ray nanospectroscopy station in experimental hutch 2, a scanning hard X-ray nanoprobe is developed for XAFS/XMCD microscopy [2]. Kirkpatric and Baez (KB) mirror optics are used to generate a circularly polarized and focused X-ray beam with a typical spot size of 100 nm × 100 nm between 5 keV and 16 keV.

An X-ray magnetic tomography technique was developed [3] to observe the three-dimensional (3D) magnetic domain structure in ferromagnetic samples. Further improvements of this technique are ongoing to enable 3D magnetic imaging under external magnetic fields with an electromagnet. The X-ray magnetic tomography technique can be applied to various ferromagnetic materials, including practical permanent magnets with sintered structures.

Time-resolved XMCD measurements with a spatial resolution of 100 nm and a time resolution of 50 ps were developed. An X-ray chopper selects X-ray pulses generated from the hybrid electron-bunch structure at SPring-8. Thus, pump-probe time-resolved measurements are feasible [4, 5]. Using this technique, element-specific and time-domain observations of the excitation of the large-amplitude spin precession in the Co/Pt multilayer in the nonlinear regime of the ferromagnetic resonance were realized [5]. This time-resolved XMCD microscopy technique will be applied to study high-frequency magnetic devices and magnetic memory devices with high-speed operations.

Naomi Kawamura, Masaichiro Mizumaki, Hitoshi Osawa, and Motohiro Suzuki

Spectroscopic Analysis Group II, Spectroscopy and Imaging Division, Center for Synchrotron Radiation Research, JASRI

References:

[1] N. Kawamura *et al.*, *J. Synchrotron Rad.* **16**, 730 (2009).

[2] M. Suzuki *et al.*, *J. Phys. Conf.* **430**, 012017 (2013).

[3] M. Suzuki *et al.*, *Appl. Phys. Express* **11**, 036601 (2018).

[4] H. Osawa *et al.*, *Jpn. J. Appl. Phys.* **56**, 048001 (2017).

[5] N. Kikuchi *et al.*, *IEEE Trans. Magn.* **54**, 6100106 (2018).